

# *SPEN* haploinsufficiency causes a neurodevelopmental disorder overlapping proximal 1p36 deletion syndrome with an epismature of X chromosomes in females

Francesca Clementina Radio,<sup>1</sup> Kaifang Pang,<sup>2,58</sup> Andrea Ciolfi,<sup>1,58</sup> Michael A. Levy,<sup>3,58</sup> Andrés Hernández-García,<sup>4</sup> Lucia Pedace,<sup>5</sup> Francesca Pantaleoni,<sup>1</sup> Zhandong Liu,<sup>2</sup> Elke de Boer,<sup>6,7</sup> Adam Jackson,<sup>8,9</sup> Alessandro Bruselles,<sup>10</sup> Haley McConkey,<sup>3</sup> Emilia Stellacci,<sup>10</sup> Stefania Lo Cicero,<sup>10</sup> Marialetizia Motta,<sup>1</sup> Rosalba Carrozzo,<sup>1</sup> Maria Lisa Dentici,<sup>1</sup> Kirsty McWalter,<sup>11</sup> Megha Desai,<sup>11</sup> Kristin G. Monaghan,<sup>11</sup> Aida Telegrafi,<sup>11</sup> Christophe Philippe,<sup>12,13</sup>

(Author list continued on next page)

## Summary

Deletion 1p36 (del1p36) syndrome is the most common human disorder resulting from a terminal autosomal deletion. This condition is molecularly and clinically heterogeneous. Deletions involving two non-overlapping regions, known as the distal (telomeric) and proximal (centromeric) critical regions, are sufficient to cause the majority of the recurrent clinical features, although with different facial features and dysmorphisms. *SPEN* encodes a transcriptional repressor commonly deleted in proximal del1p36 syndrome and is located centromeric to the proximal 1p36 critical region. Here, we used clinical data from 34 individuals with truncating variants in *SPEN* to define a neurodevelopmental disorder presenting with features that overlap considerably with those of proximal del1p36 syndrome. The clinical profile of this disease includes developmental delay/intellectual disability, autism spectrum disorder, anxiety, aggressive behavior, attention deficit disorder, hypotonia, brain and spine anomalies, congenital heart defects, high/narrow palate, facial dysmorphisms, and obesity/increased BMI, especially in females. *SPEN* also emerges as a relevant gene for del1p36 syndrome by co-expression analyses. Finally, we show that haploinsufficiency of *SPEN* is associated with a distinctive DNA methylation epismature of the X chromosome in affected females, providing further evidence of a specific contribution of the protein to the epigenetic control of this chromosome, and a paradigm of an X chromosome-specific epismature that classifies syndromic traits. We conclude that *SPEN* is required for multiple developmental processes and *SPEN* haploinsufficiency is a major contributor to a disorder associated with deletions centromeric to the previously established 1p36 critical regions.

Neurodevelopmental disorders (NDDs) and intellectual disability (ID) affect approximately 1%–3% of the general population.<sup>1–3</sup> NDDs/ID are largely genetically determined, but identification of the underlying molecular causes has been hampered by clinical and genetic heterogeneity. During the last decades, the use of high-resolution array-based copy number variant (CNV) analysis and second-generation sequencing techniques has improved our knowledge of the genetic basis of both syndromic and non-syndromic NDDs/ID.<sup>2–4</sup> Notwithstanding these

achievements, the genetic basis of NDDs/ID is still unsolved in a large proportion of affected individuals.

Deletion 1p36 (del1p36) syndrome, first described by Shapira and colleagues in 1997,<sup>5</sup> is the most common autosomal terminal deletion syndrome in humans, occurring in about 1 in 5,000 births.<sup>6–8</sup> This disorder is characterized by developmental delay (DD)/ID, behavioral abnormalities, hypotonia, seizures, brain anomalies, vision problems, hearing loss, orofacial clefting, congenital heart defects (CHDs), cardiomyopathy, renal anomalies, short

<sup>1</sup>Genetics and Rare Disease Research Division, Ospedale Pediatrico Bambino Gesù, IRCCS, 00146 Rome, Italy; <sup>2</sup>Division of Neurology and Developmental Neuroscience, Baylor College of Medicine, Houston, TX 77030, USA; <sup>3</sup>Molecular Genetics Laboratory, Molecular Diagnostics Division, London Health Sciences Centre, London, ON N6A5W9, Canada; <sup>4</sup>Department of Molecular and Human Genetics, Baylor College of Medicine, Houston, TX 77030, USA; <sup>5</sup>Oncohaematology Research Division, Ospedale Pediatrico Bambino Gesù, IRCCS, 00146 Rome, Italy; <sup>6</sup>Department of Human Genetics, Radboudumc, 6525 GA Nijmegen, the Netherlands; <sup>7</sup>Donders Institute for Brain, Cognition and Behaviour, Radboud University, 6525 GA Nijmegen, the Netherlands; <sup>8</sup>Division of Evolution & Genomic Sciences, School of Biological Sciences, Faculty of Biology, Medicine and Health, University of Manchester, M13 9 WL Manchester, UK; <sup>9</sup>Manchester Centre for Genomic Medicine, St Mary's Hospital, Manchester University NHS Foundation Trust, M13 9WL Manchester, UK; <sup>10</sup>Department of Oncology and Molecular Medicine, Istituto Superiore di Sanità, 00161 Rome, Italy; <sup>11</sup>GeneDx, Gaithersburg, MD 20877, USA; <sup>12</sup>Inserm UMR 1231 GAD (Génétique des Anomalies du Développement), Université de Bourgogne, 21070 Dijon, France; <sup>13</sup>UF Innovation en Diagnostic Génomique des Maladies Rares, CHU, Dijon Bourgogne, 21079 Dijon, France; <sup>14</sup>Division of Medical Genetics, Department of Pediatrics, Cedars Sinai Medical Center, David Geffen School of Medicine at UCLA, Los Angeles, CA 90048, USA; <sup>15</sup>Phoenix Children's Hospital, Phoenix, AZ 85016, USA; <sup>16</sup>Division of Medical Genetics, Department of Pediatrics, UPMC Children's Hospital of Pittsburgh, Pittsburgh, PA 15224, USA; <sup>17</sup>McMaster Children's Hospital, Hamilton, ON L8N 3Z5, Canada; <sup>18</sup>Clinical genetics, NYU Langone Long Island School of Medicine, Mineola, NY 11501, USA; <sup>19</sup>Center for Pediatric Genomic Medicine, Children's Mercy Hospital, Kansas City, MO 64108, USA; <sup>20</sup>Children's Hospital of Eastern Ontario, Ottawa, ON K1H 8L1, Canada; <sup>21</sup>Mendelics

(Affiliations continued on next page)



Antonio Vitobello,<sup>12,13</sup> Margaret Au,<sup>14</sup> Katheryn Grand,<sup>14</sup> Pedro A. Sanchez-Lara,<sup>14</sup> Joanne Baez,<sup>14</sup> Kristin Lindstrom,<sup>15</sup> Peggy Kulch,<sup>15</sup> Jessica Sebastian,<sup>16</sup> Suneeta Madan-Khetarpal,<sup>16</sup> Chelsea Roadhouse,<sup>17</sup> Jennifer J. MacKenzie,<sup>17</sup> Berrin Monteleone,<sup>18</sup> Carol J. Saunders,<sup>19</sup> July K. Jean Cuevas,<sup>19</sup> Laura Cross,<sup>19</sup> Dihong Zhou,<sup>19</sup> Taila Hartley,<sup>20</sup> Sarah L. Sawyer,<sup>20</sup> Fabíola Paoli Monteiro,<sup>21</sup> Tania Vertemati Secches,<sup>21</sup> Fernando Kok,<sup>21</sup> Laura E. Schultz-Rogers,<sup>22</sup> Erica L. Macke,<sup>22</sup> Eva Morava,<sup>22,23</sup> Eric W. Klee,<sup>22</sup> Jennifer Kempainen,<sup>22</sup> Maria Iascone,<sup>24</sup> Angelo Selicorni,<sup>25</sup> Romano Tenconi,<sup>26</sup> David J. Amor,<sup>27,28</sup> Lynn Pais,<sup>29</sup> Lyndon Gallacher,<sup>27,28</sup> Peter D. Turnpenny,<sup>30</sup> Karen Stals,<sup>30</sup> Sian Ellard,<sup>30</sup> Sara Cabet,<sup>31</sup> Gaetan Lesca,<sup>31</sup> Joset Pascal,<sup>32</sup> Katharina Steindl,<sup>32</sup> Sarit Ravid,<sup>33</sup> Karin Weiss,<sup>34</sup> Alison M.R. Castle,<sup>35</sup> Melissa T. Carter,<sup>35</sup> Louisa Kalsner,<sup>36</sup> Bert B.A. de Vries,<sup>6,7</sup> Bregje W. van Bon,<sup>6</sup> Marijke R. Wevers,<sup>6</sup> Rolph Pfundt,<sup>6</sup> Alexander P.A. Stegmann,<sup>6,37</sup> Bronwyn Kerr,<sup>9</sup> Helen M. Kingston,<sup>9</sup> Kate E. Chandler,<sup>9</sup> Willow Sheehan,<sup>38</sup> Abdallah F. Elias,<sup>38</sup> Deepali N. Shinde,<sup>39</sup> Meghan C. Towne,<sup>39</sup> Nathaniel H. Robin,<sup>40</sup> Dana Goodloe,<sup>40</sup> Adeline Vanderver,<sup>41,42</sup> Omar Sherbini,<sup>40</sup> Krista Bluske,<sup>43</sup> R. Tanner Hagelstrom,<sup>43</sup> Caterina Zanus,<sup>44</sup> Flavio Faletra,<sup>44</sup> Luciana Musante,<sup>44</sup> Evangeline C. Kurtz-Nelson,<sup>45</sup> Rachel K. Earl,<sup>45</sup> Britt-Marie Anderlid,<sup>46</sup> Gilles Morin,<sup>47</sup> Marjon van Slegtenhorst,<sup>48</sup> Karin E.M. Diderich,<sup>48</sup> Alice S. Brooks,<sup>48</sup> Joost Gribnau,<sup>49</sup> Ruben G. Boers,<sup>49</sup> Teresa Robert Finestra,<sup>49</sup> Lauren B. Carter,<sup>50</sup> Anita Rauch,<sup>32</sup> Paolo Gasparini,<sup>44,51</sup> Kym M. Boycott,<sup>20</sup> Tahsin Stefan Barakat,<sup>48</sup> John M. Graham, Jr.,<sup>14</sup> Laurence Faivre,<sup>52,53</sup> Siddharth Banka,<sup>8,9</sup> Tianyun Wang,<sup>54</sup> Evan E. Eichler,<sup>54,55</sup> Manuela Priolo,<sup>56</sup> Bruno Dallapiccola,<sup>1</sup> Lisenka E.L.M. Vissers,<sup>6,7</sup> Bekim Sadikovic,<sup>3,59</sup> Daryl A. Scott,<sup>4,57,59</sup> Jimmy Lloyd Holder, Jr.,<sup>2,59</sup> and Marco Tartaglia<sup>1,\*</sup>

stature, and a distinctive gestalt.<sup>8,9</sup> Further characterization has disclosed clinical and molecular heterogeneity of this disorder, and two critical regions, known as the distal (telomeric) and proximal (centromeric) critical regions, have been associated with overlapping clinical features and distinct facial characteristics.<sup>10,11</sup>

The distal critical region was first described by Wu and colleagues, who noted that 1p36 deletions have different breakpoints and most of the clinical symptoms result from haploinsufficiency of genes located distal to marker D1S2870 (chr1: 6,289,764–6,289,973; hg19).<sup>12</sup> Subsequent deletion/phenotype mapping has revealed that the cardinal features of del1p36 syndrome are seen in individ-

uals with deletions encompassing a region located within 3 Mb from the 1p telomere.<sup>10,13,14</sup> Rosenfeld and colleagues suggested that a 174 kb region at 1p36.33 could be linked to some clinical features of del1p36 syndrome.<sup>15</sup> Within this region, *GABRD* (MIM: 137163) has been implicated in the development of DD/neuropsychiatric features and seizures,<sup>16,17</sup> *PRDM16* (MIM: 605557) in the development of cardiomyopathy,<sup>18</sup> *MMP23B* (MIM: 603321) in delayed fontanel closure,<sup>13</sup> *KCNAB2* (MIM: 601142) in seizures occurrence,<sup>16,19</sup> *SKI* (MIM: 164780) in orofacial clefting,<sup>10</sup> and *PRKCZ* (MIM: 176982) in cardiovascular malformations and cardiomyopathy.<sup>20</sup> The distal critical region also includes a locus for hyperphagia and obesity.<sup>21</sup>

Genomic Analysis, Campo Belo - São Paulo 04013-000, Brazil; <sup>22</sup>Center for Individualized Medicine, Mayo Clinic, Rochester, MN 55905, USA; <sup>23</sup>Department of Clinical Genomics, Mayo Clinic, Rochester, MN 55905, USA; <sup>24</sup>Ospedale Papa Giovanni XXIII, 24127 Bergamo, Italy; <sup>25</sup>Azienda Socio Sanitaria Territoriale Lariana, 22100 Como, Italy; <sup>26</sup>Dipartimento di Pediatria, Università di Padova, 35137 Padua, Italy; <sup>27</sup>Victorian Clinical Genetics Services, Murdoch Children's Research Institute, Melbourne, VIC 3052, Australia; <sup>28</sup>Department of Paediatrics, University of Melbourne, Royal Children's Hospital, Melbourne, VIC 3052, Australia; <sup>29</sup>Medical and Populations Genetics Program, Broad Institute of MIT and Harvard, Cambridge, MA 02142, USA; <sup>30</sup>Royal Devon & Exeter NHS Foundation Trust, Exeter EX2 5DW, UK; <sup>31</sup>Department of Genetics, Hospices Civils de Lyon, Groupement Hospitalier Est, Claude Bernard Lyon 1 University, 69002 Lyon, France; <sup>32</sup>Institute of Medical Genetics, University of Zurich, 8952 Schlieren, Zurich, Switzerland; <sup>33</sup>Pediatric Neurology Unit, Ruth Children's Hospital, Rambam Health Care Campus, Haifa 3109601, Israel; <sup>34</sup>Genetics Institute, Rambam Health Care Campus, Rappaport Faculty of Medicine, Israel Institute of Technology, Haifa 3109601, Israel; <sup>35</sup>Department of Genetics, CHEO, University of Ottawa, Ottawa, ON K1N 6N5, Canada; <sup>36</sup>Connecticut Children's Medical Center, University of Connecticut School of Medicine, Farmington, CT 06032, USA; <sup>37</sup>Department of Clinical Genetics, Maastricht University Medical Center+, 6229 HX Maastricht, the Netherlands; <sup>38</sup>Department of Medical Genetics, Shodair Children's Hospital, Helena, MT 59601, USA; <sup>39</sup>Ambry Genetics, Aliso Viejo, CA 92656, USA; <sup>40</sup>Department of Genetics, University of Alabama at Birmingham, Birmingham, AL 35294, USA; <sup>41</sup>Division of Neurology, Children's Hospital of Philadelphia, Philadelphia, PA 19104, USA; <sup>42</sup>Department of Neurology, Perelman School of Medicine, University of Pennsylvania, Philadelphia, PA 19104, USA; <sup>43</sup>Illumina Clinical Services Laboratory, San Diego, CA 92122, USA; <sup>44</sup>Institute for Maternal and Child Health, IRCCS "Burlo Garofolo," 34137 Trieste, Italy; <sup>45</sup>Department of Psychiatry & Behavioral Sciences, University of Washington, Seattle, WA 98195, USA; <sup>46</sup>Department of Molecular Medicine and Surgery, Karolinska Institutet and Department of Clinical Genetics, Karolinska University Hospital, 17176 Stockholm, Sweden; <sup>47</sup>CA de Génétique Clinique & Oncogénétique, CHU Amiens-Picardie, 80054 Amiens, France; <sup>48</sup>Department of Clinical Genetics, Erasmus MC University Medical Center, 3015 GD Rotterdam, the Netherlands; <sup>49</sup>Department of Developmental Biology, OncoCode Institute, Erasmus MC, University Medical Center, 3015 GD Rotterdam, the Netherlands; <sup>50</sup>Department of Pediatrics, Division of Medical Genetics, Levine Children's Hospital Atrium Health, Charlotte, NC 28203, USA; <sup>51</sup>Department of Medicine, Surgery & Health Science, University of Trieste, 34143 Trieste, Italy; <sup>52</sup>Centre de Référence Maladies Rares « Anomalies du Développement et Syndromes Malformatifs », Centre de Génétique, FHU-TRANSLAD et Institut GIMI, 77908 Dijon, France; <sup>53</sup>UMR 1231 GAD, Inserm - Université Bourgogne-Franche Comté, 77908 Dijon, France; <sup>54</sup>Department of Genome Sciences, University of Washington School of Medicine, Seattle, WA 98195, USA; <sup>55</sup>Howard Hughes Medical Institute, University of Washington, Seattle, WA 98195, USA; <sup>56</sup>UOSD Genetica Medica del Grande Ospedale Metropolitano "Bianchi Melacrino Morelli" di Reggio Calabria, 89124 Reggio Calabria, Italy; <sup>57</sup>Department of Molecular Physiology and Biophysics, Baylor College of Medicine, Houston, TX 77030, USA

<sup>58</sup>These authors contributed equally

<sup>59</sup>These authors contributed equally

\*Correspondence: marco.tartaglia@opbg.net

<https://doi.org/10.1016/j.ajhg.2021.01.015>



The proximal critical region was refined by Kang and colleagues,<sup>11</sup> who described five subjects with interstitial 1p36 deletions (Figure 1A). One of these individuals had many features suggestive of del1p36 syndrome, although the deletion did not include the distal critical region (chr1: 8,395,179–11,362,893; hg19). This subject, and

**Figure 1. Known critical regions at 1p36, deletions involving *SPEN*, and facial features of subjects with *de novo* truncating *SPEN* variants**

(A) Cartoon showing the distal and proximal del1p36 critical regions (red boxes) as defined by Wu et al.<sup>12</sup> and Kang et al.<sup>11</sup> and Jordan et al.,<sup>14</sup> respectively. Deletions shown by Kang et al.<sup>11</sup> and Rudnik-Schöneborn et al.<sup>22</sup> (estimated on the basis of the data provided) to characterize the phenotypes associated with the proximal 1p36 critical region are shown as orange bars. One of these deletions does not include *RERE*, and three of these deletions include *SPEN* (green bars). Previously reported deletions that overlap *SPEN* and at least one of the critical regions are shown as blue bars. Deletions that affect *SPEN* but do not include either the distal or proximal 1p36 critical regions are shown as black bars.

(B) Facial features of subjects with truncating variants in *SPEN*. Note the occurrence of broad forehead with frontal bossing, bitemporal narrowing, wide set eyes, arched (childhood) and long bushy (adulthood) eyebrows, synophrys, dysplastic overfolded ears with uplifted ear lobe, wide and depressed nasal bridge, broad nose with prominent/bulbous nasal tip, anteverted nares, long philtrum with thick vermilion, high/narrow palate without cleft, and pointed/rounded chin. A detailed clinical characterization of affected subjects is reported in Table S2 and Supplemental notes.

others with overlapping deletions, had distinct facial features compared to individuals with distal 1p36 deletions.<sup>11,20,22</sup> Within this region, haploinsufficiency of *RERE* (MIM: 605226), which encodes a nuclear receptor coregulator,<sup>23</sup> has been shown to underlie a neurodevelopmental disorder whose cardinal features overlap, in part, those associated with deletions of the proximal critical region.<sup>24,25</sup> So far, haploinsufficiency of other genes in the proximal 1p36 critical region has not been associated with the development of clinically significant phenotypes.

Individuals with interstitial deletions of 1p36.21p36.13 not overlapping with either the distal or proximal 1p36 critical region have been reported to have phenotypes similar to those seen in association with deletion of the distal and proximal 1p36 critical regions (Figure 1A). This finding suggests that haploinsufficiency of genes located centromeric to the two critical regions plays a significant role in the disease.

The *Drosophila* split ends homolog gene, *SPEN* (MIM: 613484), also known as MSH2-interacting nuclear target (*MINT*) and SMART/HDAC1-associated repressor protein (*SHARP*), is located on chromosome 1p36.21p36.13 and is centromeric to the proximal 1p36 critical region (Figure 1A). *SPEN* encodes a large protein (approximately 400 kDa) characterized by four putative RNA recognition motifs (RRMs) at the N terminus, multiple nuclear localization signals spaced throughout the molecule, a nuclear receptor interaction domain (RID), and a Spen paralog and ortholog

C-terminal (SPOC) domain mediating protein-protein interactions at the C terminus. SPEN functions as a transcriptional repressor through interactions with other repressors and chromatin-remodeling complexes, including histone deacetylases (HDACs), or by sequestering transcriptional activators.<sup>26–29</sup> SPEN regulates stem cell self-renewal and differentiation,<sup>30</sup> is frequently mutated in human cancers,<sup>31,32</sup> and also plays a critical role during embryogenesis and throughout development by regulating cell fate and differentiation through its modulation of Notch, T-cell factor/lymphoid enhancer factor (TCF/LEF), and epidermal growth factor (EGF) signaling.<sup>33–37</sup> SPEN is required in several developmental pathways, as highlighted by the lethality/severe developmental anomalies found in animal models.<sup>33,38–40</sup> In addition, a conditional knockout of *Spn* has been related to severely underdeveloped postnatal brain in mice, indicating a role for this protein in neuronal cell development and/or survival.<sup>41</sup> SPEN is deleted in a subset of subjects with proximal 1p36 deletions, and large cohort studies have previously indicated a role of deleterious SPEN variants in ID and autism spectrum disorder (ASD),<sup>42–47</sup> though detailed clinical information was not provided. SPEN's role in human diseases is also supported by data from the gnomAD that indicate that SPEN is highly loss-of-function (LoF) intolerant (pLI = 1; o/e = 0.03).

Here, we report that *de novo* truncating variants in SPEN underlie a recognizable syndromic NDD characterized by DD/ID, hypotonia, behavior abnormalities, multiple congenital anomalies, and facial dysmorphisms overlapping the clinical phenotype previously associated with 1p36 proximal deletions. Obesity and increased BMI, mainly in females, are also part of this disorder. Finally, we demonstrate that haploinsufficiency of SPEN is associated with a distinctive X chromosome epismutation in affected females. These findings support the role of SPEN in multiple developmental processes and indicate that SPEN haploinsufficiency is a major contributor to the phenotype caused by interstitial deletions located centromeric to the distal and proximal 1p36 critical regions.

All subjects were analyzed in the context of research projects dedicated to undiagnosed individuals or individuals referred for genetic testing. Clinical investigations were conducted according to Declaration of Helsinki principles and approved by the local institutional ethical committees. Clinical data, photographs, DNA specimens, and other biological material were collected, used, and stored after obtaining signed informed consents from the participating subjects/families. We were granted permission to publish the photographs of all subjects shown in Figure 1B. Genomic analyses were performed with DNA samples obtained from leukocytes. Target enrichment kits and whole-exome sequencing (WES) statistics are reported in Table S1. WES data processing, including sequence alignment to GRCh37/GRCh38, and variant filtering and prioritization by allele frequency, predicted functional impact, and inheritance were performed as pre-

viously reported.<sup>42,47–58</sup> Variants' validation and segregation analyses were carried out by Sanger sequencing.

Subject 1, an individual with a molecularly unexplained condition with clinical features suggestive of the phenotype associated with proximal 1p36 deletions (Figure 1B, Table S2, Supplemental notes), was found to be negative for chromosomal structural rearrangements by high-resolution SNP array analysis. WES data analysis did not find functionally relevant variants in genes previously associated with Mendelian disorders on the basis of the expected inheritance model and clinical presentation. However, we identified a *de novo* truncating variant in SPEN (c.6058C>T [p.Gln2020\*]; GenBank: NM\_015001.3). This was particularly intriguing given the SPEN's location on chromosome 1p36 (chr1: 16,174,359–16,266,955; hg19). This led us to hypothesize that haploinsufficiency of SPEN might contribute to the phenotypes associated with interstitial deletions located centromeric to the distal and proximal 1p36 critical regions.

To test this hypothesis, we used GeneMatcher<sup>59</sup> and data from DECIPHER<sup>60</sup> to accrue a cohort of an additional 33 individuals (subjects 2–34) with truncating variants in SPEN (Table 1, Figure 1B). A detailed clinical description of each subject is reported in the supplemental information (Table S2, Supplemental notes). In all affected individuals, the truncating SPEN variant was considered the best disease-causing candidate. None of the identified variants had been reported in gnomAD, and sequencing of DNA obtained from fibroblasts in three subjects confirmed the presence of the variant, strongly supporting their germline origin.

Overall, the phenotypes of these subjects showed significant overlap with those commonly associated with deletions of the distal and proximal 1p36 critical regions (Table 2). The main features included DD/ID, behavioral and/or psychiatric disorders, brain anomalies, CHDs, high/narrow palate, facial dysmorphisms, and obesity/elevated BMI more common in females. DD/ID ranged from mild to severe, and language delay was invariably present. Behavioral and/or psychiatric features (i.e., ASD, anxiety, aggressive behavior, and attention deficit disorder) were noted in a high proportion of subjects (81%). Brain/spine imaging was available in 22 affected individuals, and major anomalies were detected in 14 (64%) of them. In particular, polymicrogyria, heterotopia, cerebellar atrophy, anomalies of periventricular white matter, corpus callosum agenesis, and tethered cord were documented (Table S2, Supplemental notes). Other common neurologic findings included generalized hypotonia (73%), oral motor hypotonia (43%), gait imbalance (48%), and abnormal pyramidal signs (25%). Seizures were reported in three subjects. Two of these individuals had normal brain MRIs and one was not assessed for brain anomalies.

A significant proportion of the subjects had CHDs (28%). Ventricular septal defects, patent foramen ovale, patent ductus arteriosus, and mitral regurgitation were particularly common. The craniofacial appearance included broad forehead (26%) with frontal bossing (16%), bitemporal narrowing (39%), arched elongated

**Table 1. List of the identified truncating SPEN mutations**

Nucleotide change	Amino acid change	gnomAD	Domain	Affected individual(s)	Origin
c.1603C>T	p.Arg535*	–	RRM4	s16	<i>de novo</i>
c.2014C>T	p.Arg672*	–	–	s4	<i>de novo</i>
c.2101G>T	p.Glu701*	–	–	s30	<i>de novo</i>
c.2262_2265dupGCTT	p.Tyr756Alafs*13	–	–	s27	unknown <sup>a</sup>
c.2269_2272dupAGCC	p.Arg758Glnfs*11	–	–	s24	<i>de novo</i>
c.2956_2959dupAGGC	p.Arg987Glnfs*36	–	–	s20	<i>de novo</i>
c.3029dupA	p.Asp1011Glyfs*11	–	–	s33	<i>de novo</i>
c.3199C>T	p.Gln1067*	–	–	s32	<i>de novo</i>
c.3508C>T	p.Arg1170*	–	–	s31	<i>de novo</i>
c.3793C>T	p.Arg1265*	–	–	s10, s13	<i>de novo</i>
c.5013_5017delGAAGA	p.Glu1671Aspfs*16	–	–	s23	<i>de novo</i>
c.5392C>T	p.Gln1798*	–	–	s34	presumed <i>de novo</i> <sup>b</sup>
c.5414delT	p.Leu1805*	–	–	s26	<i>de novo</i>
c.5806C>T	p.Arg1936*	–	–	s6	familial <sup>c</sup>
c.6058C>T	p.Gln2020*	–	–	s1	<i>de novo</i>
c.6087_6088delAC	p.Glu2029Aspfs*5	–	–	s2	<i>de novo</i>
c.6223_6227delTCAAA	p.Ser2075Glnfs*46	–	–	s8	<i>de novo</i>
c.6226_6227delAA	p.Lys2076Glnfs*46	–	–	s11	<i>de novo</i>
c.6570dupT	p.Lys2191*	–	–	s17	<i>de novo</i>
c.6641_6642delAG	p.Glu2214Alafs*11	–	RID	s28	<i>de novo</i>
c.6799G>T	p.Glu2267*	–	RID	s29	presumed <i>de novo</i> <sup>d</sup>
c.6974_6975delTT	p.Leu2325Argfs*33	–	RID	s12	<i>de novo</i>
c.7024C>T	p.Arg2342*	–	RID	s9	<i>de novo</i>
c.7324G>T	p.Glu2442*	–	RID	s5	<i>de novo</i>
c.7328delA	p.Glu2443Glyfs*17	–	RID	s18, s19	familial (2 affected siblings) <sup>e</sup>
c.7338_7339dupCA	p.Arg2447Thrfs*14	–	RID	s3	<i>de novo</i>
c.7373delC	p.Pro2458Argfs*2	–	RID	s15	<i>de novo</i>
c.7374_7381delGGTGACCC	p.Val2459Thrfs*36	–	RID	s14	<i>de novo</i>
c.7492delG	p.Val2498*	–	RID	s7	<i>de novo</i>
c.9950dupC	p.Ala3318Glyfs*30	–	–	s21	<i>de novo</i>
c.10909_10910delAG	p.His3638Profs*7	–	SPOC	s22	<i>de novo</i>
c.10953dupC	p.Asn3652Glnfs*17	–	SPOC	s25	<i>de novo</i>

All variants have been submitted to ClinVar (ClinVar: SCV001468518–SCV001468547) or DECIPHER (DECIPHER: 280862 and 286415).

<sup>a</sup>Parental DNA specimens were not available for testing.

<sup>b</sup>The father was confirmed negative for the variant, while the mother was not available for testing.

<sup>c</sup>Inherited from the affected mother.

<sup>d</sup>The mother was confirmed negative for the variant, while the father was not available for testing.

<sup>e</sup>Inherited from the affected father.

eyebrows (39%) becoming often bushy with age, synophrys (33%), wide set eyes/telecanthus (26%), epicanthus (39%), dysplastic, uplifted or over-folded ears (35%), and broad nose with bulbous/prominent nasal tip (52%). Long philtrum, thin upper lip, teeth abnormalities, high palate, and short and/or pointed chin were also observed in several individuals. Precocious puberty was found in a

subset of subjects (28%). Obesity and increased BMI were noted in many individuals (Figure S1). Among the 31 subjects for whom BMI was assessed (Table S2), there was a statistically significant higher prevalence of obese females (6/16) compared to males (0/15) (Fisher's exact test = 0.018,  $p < 0.05$ ), and an increased BMI was generally more common in females (10/16) compared to males

**Table 2. Clinical features of subjects with truncating variants in *SPEN* and deletions encompassing *SPEN***

Subjects	<i>SPEN</i> LoF cohort	1p36 proximal deletions including <i>SPEN</i> <sup>a</sup>	1p36 proximal deletions not including <i>SPEN</i> <sup>b</sup>	Distal del1p36 syndrome <sup>c</sup>
Sex	17 female, 17 male	5 female, 5 male, 1 unknown	2 female, 5 male	N/A
Age at last exam	fetus–24 years 6 months	2 months–3 years	2–20 years	N/A
Pregnancy history complication <sup>d</sup>	19/34 (56%)	2/4 (50%)	3/6 (50%)	frequent (IUGR)
<b>Growth</b>				
Height	N/A	N/A	short stature	short stature, frequent
Weight	obesity	N/A	obesity	obesity 5/46 (10%)
OFC <sup>e</sup>	microcephaly, rare	microcephaly, rare	microcephaly, rare	microcephaly, 48/70 (68%)
Craniofacial features	high anterior hairline, bitemporal narrowing, arched/sparse eyebrow, synophrys, wide set eyes/telecanthus, epicanthus, uplifted earlobe and slightly over-folded superior helices, prominent nasal tip, flattened nasal bridge, bulbous nose, anteverted nares, long philtrum with thick vermilion, teeth abnormalities, micrognathia, high/narrow palate, and pointed chin	abnormal frontal hairline, bitemporal narrowing, frontal bossing, ridging of the metopic suture, sparse/arched eyebrow, synophrys, wide set eyes/telecanthus, epicanthus, ptosis, small palpebral fissures, upslanting palpebral fissures, low-set ears, uplifted and large earlobe, slightly over-folded superior helices, prominent nasal tip, flattened nasal bridge, bulbous nose with anteverted nares, thin upper lip, micrognathia, high/narrow palate, and pointed chin	late-closing anterior fontanel, low frontal hairline, bitemporal narrowing, sparse/arched eyebrow, straight eyebrows, synophrys, prominent eyelashes, wide set eyes/telecanthus, epicanthus, small palpebral fissures, upslanting palpebral fissures, low-set ears, slightly over-folded superior helices, prominent nasal tip, flattened nasal bridge, bulbous nose with anteverted nares, thin upper lip, teeth anomalies, high/narrow palate, and pointed chin	late-closing anterior fontanel, frontal bossing, epicanthus, small palpebral fissures, upslanting palpebral fissures, low-set ears with slightly over-folded superior helices, flattened nasal bridge, bulbous nose with anteverted nares, choanal atresia, long philtrum with thin upper lip, cleft lip/cleft palate, high/narrow palate, and pointed chin
<b>Cognition and behavior</b>				
Global developmental delay/intellectual disability	33/33 (100%)	11/11 (100%)	6/6 (100%)	157/157 (100%)
Abnormal behavior, aggressive/self-injurious behavior	22/30 (73%)	2/2 (100%)	4/4 (100%)	35/75 (47%)
ASD	18/28 (64%)	N/A	2/2 (100%)	10/37 (27%)
Stereotypic behavior	13/28 (46%)	N/A	1/1 (100%)	N/A
<b>Neurological features</b>				
Hypotonia	22/30 (73%)	3/5 (60%)	2/2 (100%)	186/202 (92%)
Oral motor hypotonia <sup>f</sup>	12[1]/28 (43%[46%])	1/1 (100%)	N/A	N/A
Seizures	3/32 (9%)	4/6 (66%)	3/5 (60%)	120/197 (61%)
Abnormal pyramidal signs	6/24 (25%)	N/A	N/A	N/A
Gait imbalance	14/27 (52%)	N/A	2/2 (100%)	N/A
CNS anomalies	14/22 (64%)	3/4 (75%)	0/1 (0%)	97/141 (69%)

(Continued on next page)

**Table 2. Continued**

Subjects	SPEN LoF cohort	1p36 proximal deletions including SPEN <sup>a</sup>	1p36 proximal deletions not including SPEN <sup>b</sup>	Distal del1p36 syndrome <sup>c</sup>
Cardiac features/CHD	14/22 (64%)	5/6 (83%)	2/3 (66%)	130/198 (66%)
GI features	13/31 (42%)	3/4 (75%)	N/A	35/107 (33%)
Ocular involvement	6/30 (20%)	1/1 (100%)	N/A	56/120 (47%)
<b>Musculoskeletal anomalies</b>				
Brachydactyly	5/30 (17%)	1/2 (50%)	0/1 (0%)	55/108 (51%)
Toes abnormalities	4/27 (15%)	1/2 (50%)	N/A	48/60 (80%)
Scoliosis/kyphosis <sup>d</sup>	5[1]/28 (18%[21%])	2/2 (100%)	N/A	12/48 (25%)
<b>Other</b>				
Feeding/swallowing problems	8/30 (27%)	4/4 (100%)	3/3 (100%)	87/125 (70%)
Hearing loss	3/31 (10%)	2/3 (66%)	1/1 (100%, conductive)	91/161 (56%)
Vascular abnormalities	9/27 (33%)	N/A	N/A	N/A
Dry skin	6/29 (21%)	N/A	N/A	N/A
Precocious puberty	4/18 (22%)	N/A	N/A	1/3 (33%)

The prevalence of individual features is compared to subjects with proximal or distal 1p36 deletions.

<sup>a</sup>This group includes subjects with deletions of variable size encompassing *SPEN*. The cohort includes previously published and publicly available cases (see “DECIPHER” in [web resources](#)) carrying 1p36 proximal deletions encompassing both the 1p36 proximal critical region and *SPEN*, not including the distal critical region. See Kang et al., 2007 (s1, s2, and s3);<sup>11</sup> Rudnik-Schöneborn et al., 2008;<sup>22</sup> Shimada et al., 2015 (s50);<sup>8</sup> Zaveri et al., 2014 (s7);<sup>20</sup> and DECIPHER (DECIPHER: 254939, 283960, 337264, 337557, and 402221).

<sup>b</sup>Subjects with deletions not including the distal 1p36 region: this cohort includes published cases carrying 1p36 proximal deletions encompassing the proximal critical region, not including the distal critical region and *SPEN* gene. See Kang et al., 2007 (s4 and s5)<sup>11</sup> and Rosenfeld et al., 2010 (s1–s4).<sup>15</sup>

<sup>c</sup>Prevalence of individual features is based on the data reported by Heilstedt et al., 2003b;<sup>10</sup> Gajicka et al., 2007;<sup>13</sup> Battaglia et al., 2008;<sup>9</sup> and Shimada et al., 2015.<sup>8</sup>

<sup>d</sup>Pregnancy history complications include intrauterine growth retardation (IUGR), increased nuchal translucency, polyhydramnios, decreased fetal movements, and preterm labor (see [Table S2](#)).

<sup>e</sup>Microcephaly is defined as occipitofrontal circumference (OFC) more than two standard deviations below the mean value for age and sex.

<sup>f</sup>Brackets indicate feeding/swallowing difficulties with a suspected defect in oral muscles without diagnosis of oral motor hypotonia.

<sup>g</sup>Brackets indicate a scoliotic/kyphotic attitude without skeletal X-ray confirmation.

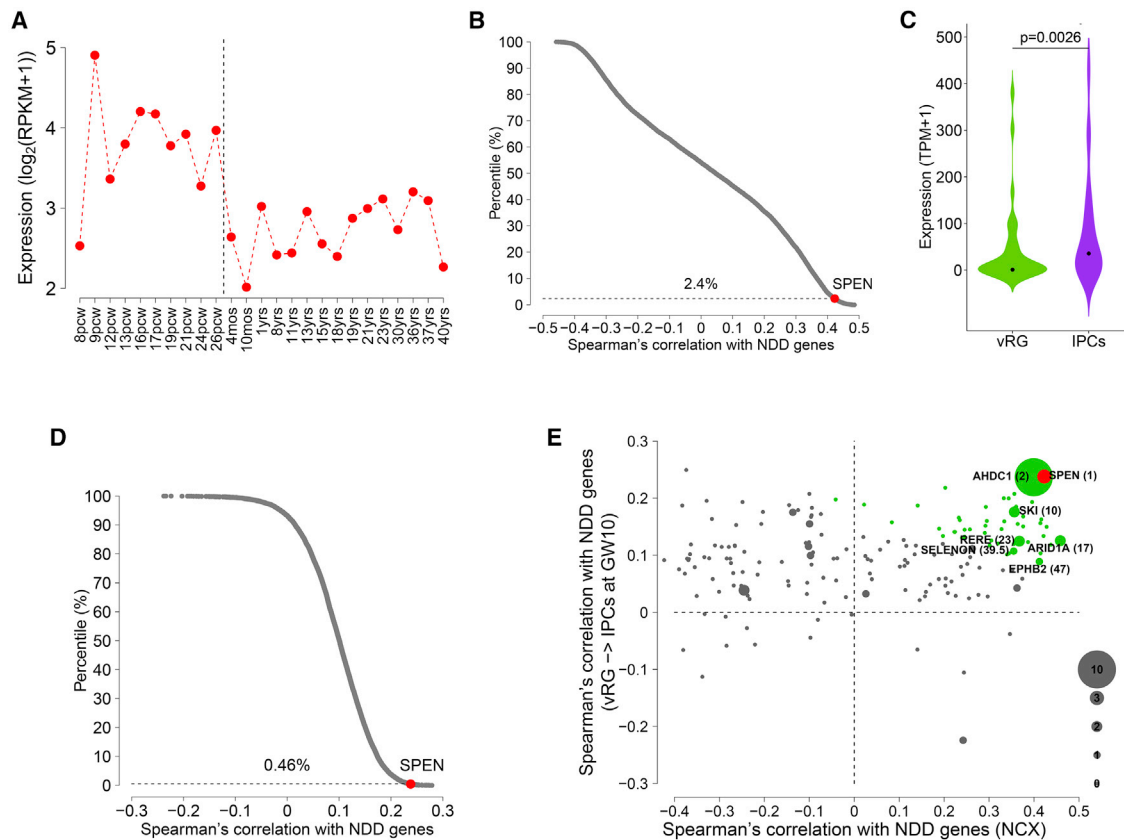


**Figure 2. *SPEN* is a critical gene for 1p36 deletion syndrome**

(A) Expression of *SPEN* during human neocortical development. The expression values of *SPEN* across cortical samples are grouped and sorted by developmental time points.

(B) Scatterplot shows the distribution of Spearman's correlation with NDD genes in cortical samples for all the genes expressed in human cortex. Dots represent individual genes. The dashed horizontal line at 2.4% indicates the top percentile among which the correlation between NDD genes and *SPEN* is ranked.

(C) Expression of *SPEN* in ventricular radial glia (vRG) cells and intermediate progenitor cells (IPCs) at gestational week 10. Violin plot shows the median value (point). p value indicates expression difference (one-sided Wilcoxon rank-sum test).

(D) Scatterplot shows the distribution of Spearman's correlation with NDD genes in the vRG-to-IPC transition at gestational week 10 for all the genes expressed in neural progenitor cells. Dots represent individual genes. The dashed horizontal line at 0.46% indicates the top percentile among which the correlation between NDD genes and *SPEN* is ranked.

(E) Scatterplot shows Spearman's correlation with NDD genes in bulk cortical samples versus the vRG-to-IPC transition for all the genes within the 1p36 region that are expressed in both conditions. Dots represent individual genes. Dot size of a gene is proportional to the number of *de novo* loss-of-function mutations for the gene in NDDs. Red denotes *SPEN* with rank 1 and green denotes genes with ranks 2 to 50. Genes ranked within top 50 and harboring at least one *de novo* loss-of-function mutation are labeled along with the corresponding ranks shown in parentheses. GW, gestational week; IPCs, intermediate progenitor cells; mos, months; NCX, neocortex; NDD, neurodevelopmental disorder; pcw, postconceptional weeks; vRG, ventricular radial glia.

(3/15) (Yates corrected  $\chi^2 = 4.130$ ,  $p = 0.042$ ). The prevalence of obesity/elevated BMI increased with age; BMI was generally reported within the normal range until age of 4 years and rose significantly thereafter.

The identified truncating *SPEN* variants were distributed throughout the coding region of the gene. A comparison of the clinical features among subjects, taking into account the location of individual variants, did not reveal significant genotype-phenotype correlations. Notably, subjects with truncating variants at the C terminus did not show a less severe phenotype, suggesting the requirement of the SPOC domain for *SPEN* function. The absence of any obvious genotype-phenotype correlations in these subjects points to a homogeneous LoF role of mutations, indicating

haploinsufficiency of *SPEN* as the mechanism of disease. This is further supported by the observation that these subjects clinically overlap with individuals presenting with interstitial deletions involving *SPEN* (Table 2).

To further evaluate *SPEN* as a candidate gene contributing to neurodevelopmental traits, we performed bioinformatic analyses to determine whether *SPEN* is co-expressed with high-confidence genes in NDDs (Supplemental methods). First, using the developing human brain RNA sequencing data,<sup>61</sup> we found that the expression of *SPEN* decreases across cortical development (Figure 2A), suggesting that *SPEN* might play a more important role during prenatal cortical development than postnatally. We also found that *SPEN* exhibits highest expression



around postconceptional week 9 (Figure 2A), suggesting that the protein could have an important function around this developmental time. We then calculated the Spearman's correlation with genes associated with NDDs for all the genes expressed in human cortex and found that *SPEN* is highly positively correlated with NDD genes (Figure 2B, Table S3). Next, using the single-cell RNA sequencing data from the developing human prefrontal cortex,<sup>62</sup> we found that the expression of *SPEN* significantly increases during the transition from ventricular radial glia (vRG) cells to intermediate progenitor cells (IPCs) at gestational week 10 (Figure 2C), a key point of gene convergence in NDDs.<sup>63</sup> We then calculated the Spearman's correlation with genes associated with NDDs for all the genes expressed in neural progenitor cells and found that *SPEN* is highly positively correlated with NDD genes during the transition (Figure 2D, Table S4), implicating that *SPEN* could function together with other NDD genes to promote this neural progenitor cell transition. Because NDD genes show high co-expression convergence in cortical development,<sup>63–66</sup> the high correlation scores with NDD genes for *SPEN* further support its functional relevance in neurodevelopmental processes. By combining the two types of Spearman's correlation from the bulk tissue and single-cell data together, *SPEN* ranked first among all the genes within chromosome 1p36 (Figure 2E, Table S5), strongly pointing to it as a critical gene for proximal del1p36 syndrome.

A role for *SPEN* in chromatin remodeling has been reported.<sup>27–29,67,68</sup> On the basis of these considerations, we performed a genome-wide methylation profiling analysis to investigate possible perturbations at the epigenome level associated with *SPEN* haploinsufficiency. We used the Infinium Human MethylationEPIC BeadChip assay (Illumina) to allow comprehensive genome-wide coverage. Peripheral blood DNA was available from a subset of 11 subjects with truncating *SPEN* variants and seven age-matched “batch” control individuals of European descent, which we processed across four batches to reduce any batch effect. Twenty-two additional “cohort” control individuals that had been processed separately were also included. Bisulfite conversion and hybridization workflow were performed according to the manufacturer's protocol. Data analysis was carried out as previously described (Supplemental methods).<sup>69,70</sup> After filtering, we used 776,314 probes to compare the methylation profile of the subjects with truncating *SPEN* variants with control individuals. Considering the entire set of assayed target probes, the analysis did not highlight a substantial change in methylation pattern (data not shown), indicating that *SPEN* haploinsufficiency does not significantly impact the global methylation status of the genome. We then sought to identify a set of individual probes that could differentiate samples with *SPEN*-truncating mutations from control samples. We identified 418 autosomal probes that fulfilled our criteria based on methylation change, p value, receiver operator characteristic (ROC) metrics, and correla-

tion filtering (Supplemental methods). Hierarchical clustering and multidimensional scaling (MDS) analysis showed that the training set of samples with a *SPEN*-mutated allele clustered separately from the controls (Figures S2A and S2B). Cross-validation analysis confirmed the epismature in the training set (Figure S3), although it was not robust enough to overcome batch effects when tested via an independent cohort of controls processed in the same lab (OPBG, Rome, Italy) or in other reference control samples within the EpiSign Knowledge Database (LHSC/WU, London, Canada) (Figures S2C and S2D). Given the role of *SPEN* in X chromosome inactivation and X-linked gene silencing,<sup>28,68,71</sup> we then wondered whether *SPEN* haploinsufficiency could cause methylation changes on the X chromosome in female individuals. We repeated the DNA methylation analysis focusing on the X chromosome (17,308 probes) in samples from females (7 affected individuals and 6 batch-matched control individuals). 122 probes met significance filtering criteria based on methylation change, p value, ROC, and correlation filtering. This probe set separated subjects with truncating *SPEN* variants from control samples in two distinct clusters (Figures 3A). The epismature identified in the training set (Table S6) was cross validated (Figure S4). Adding *SPEN*-mutated and control male samples to the tested cohort allowed us to successfully differentiate *SPEN*-mutated females from control samples but not *SPEN*-mutated males from controls (Figure 3B). The support vector machine (SVM) classifier, when applied to females with *SPEN* mutations and control samples, confirmed the ability of the X chromosome epismature to properly classify samples and controls (Figure 3C). We then applied the *SPEN* X chromosome epismature to approximately 500 samples from female subjects affected by 38 syndromes exhibiting 32 different epismatures to test its specificity.<sup>70</sup> We used female *SPEN* mutation-positive samples and batch controls along with 75% of the other controls and samples from other NDDs to train the SVM classifier. The remaining 25% of samples were reserved for testing. All of the other NDD samples and controls had low probability scores, indicating that the classifier can successfully differentiate between females with *SPEN* mutations and other epismature positive NDDs and unaffected individuals (Figure 4).

Here, we established that truncating mutations in *SPEN* cause a recognizable NDD with a characteristic X chromosome epismature in females. The consistent phenotype of this condition includes DD/ID, hypotonia, behavior abnormalities, multiple congenital anomalies mainly involving brain and heart, and facial dysmorphisms (i.e., broad forehead; arched and long eyebrows, frequently bushy in adulthood; posteriorly rotated and dysmorphic ears; wide and depressed nasal bridge; nose with bulbous/prominent tip and anteverted nares; long philtrum with thick vermilion; high/narrow palate; and rounded/pointed chin). *SPEN* is centromeric to the proximal 1p36 critical region and most likely a major contributor to the

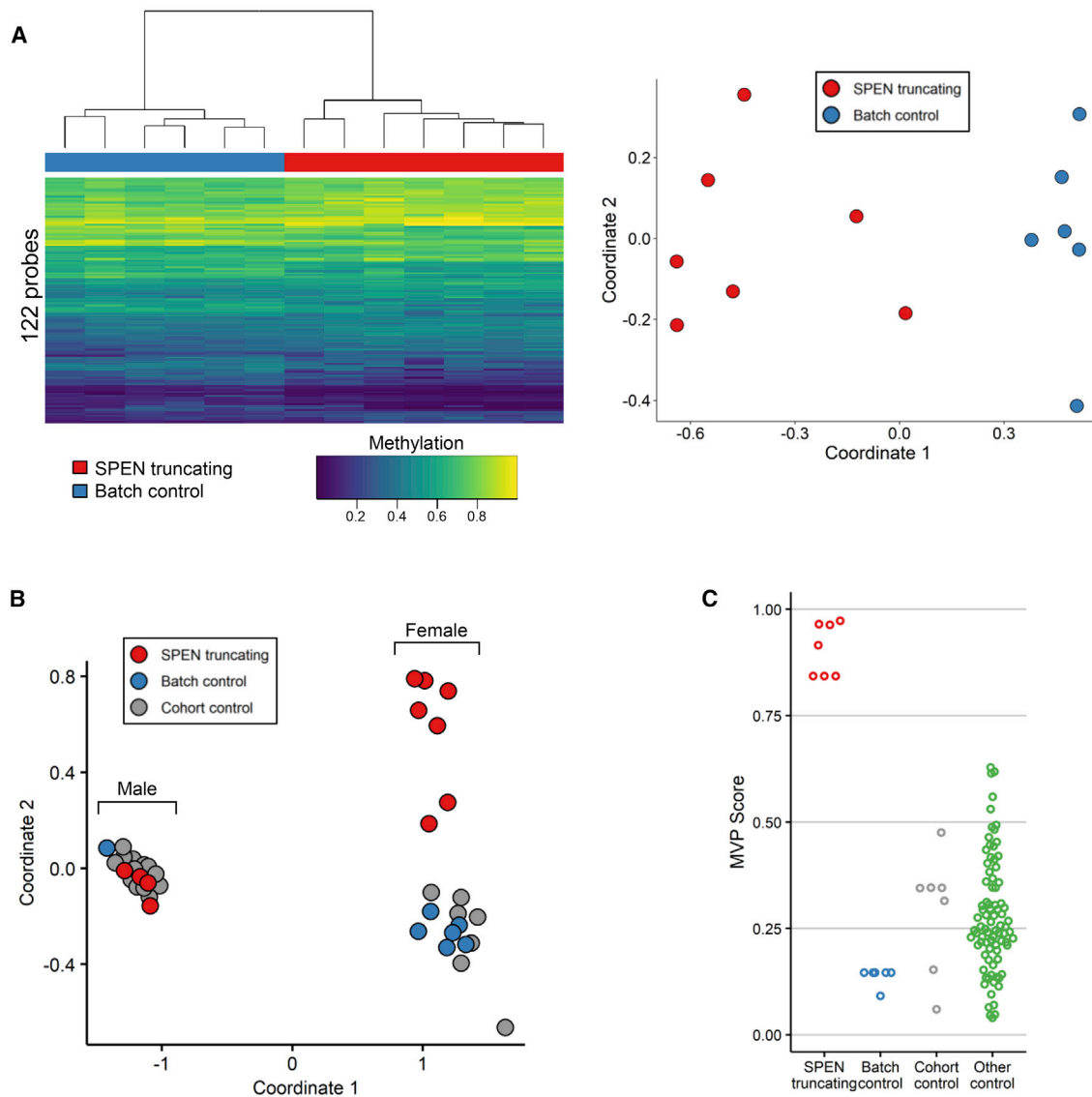


### Figure 3. Female subjects with *SPEN*-truncating mutations exhibit an X chromosome-specific epigenature

(A) Samples from female individuals were compared to samples from healthy female control individuals processed alongside the *SPEN*-mutated samples (batch controls) and CpGs on the X chromosome were analyzed. The epigenature was able to separate *SPEN*-truncated samples from control individuals as shown by hierarchical clustering (left) and multidimensional scaling (right) analyses.

(B) The X chromosome epigenature was able to differentiate between females with *SPEN* mutations and control samples but not between males with *SPEN* mutations and control samples.

(C) Support vector machine-based methylation variant pathogenicity (MVP) scores showed that the X chromosome signature scored female samples differently from all the other tested samples.

phenotypes seen in individuals with proximal 1p36 deletions encompassing 1p36.21p36.13.

The “classical” distal del1p36 syndrome and “proximal” del1p36 syndrome are both characterized by DD/ID and a variable constellation of congenital defects (e.g., central nervous system anomalies, cleft palate/narrow palate, CHDs, and kidney disease) (Table 2). Our findings provide evidence for the existence of a third centromeric region implicated in human disease and defining a clinical entity linked to deletions of 1p36.21p36.13.

Comparison of facial features of subjects with truncating *SPEN* mutations with those observed in individuals with distal del1p36 syndrome (Table 2) clinically splits these

two conditions. Although both disorders share some common nonspecific features (e.g., epicanthus, low set ears, broad/flattened nasal bridge, long philtrum, and pointed chin), distal del1p36 syndrome is well defined by frequently occurring distinctive facial features (i.e., straight eyebrows, deep set eyes, hypotelorism, and midface hypoplasia) that are rarely found in subjects with *SPEN* haploinsufficiency, who rather show some of the facial characteristics found in individuals with proximal 1p36 deletions also including *SPEN*.

A remarkable finding of the present study was the frequent occurrence of obesity/increased BMI in subjects with truncating *SPEN* mutations, with a significant

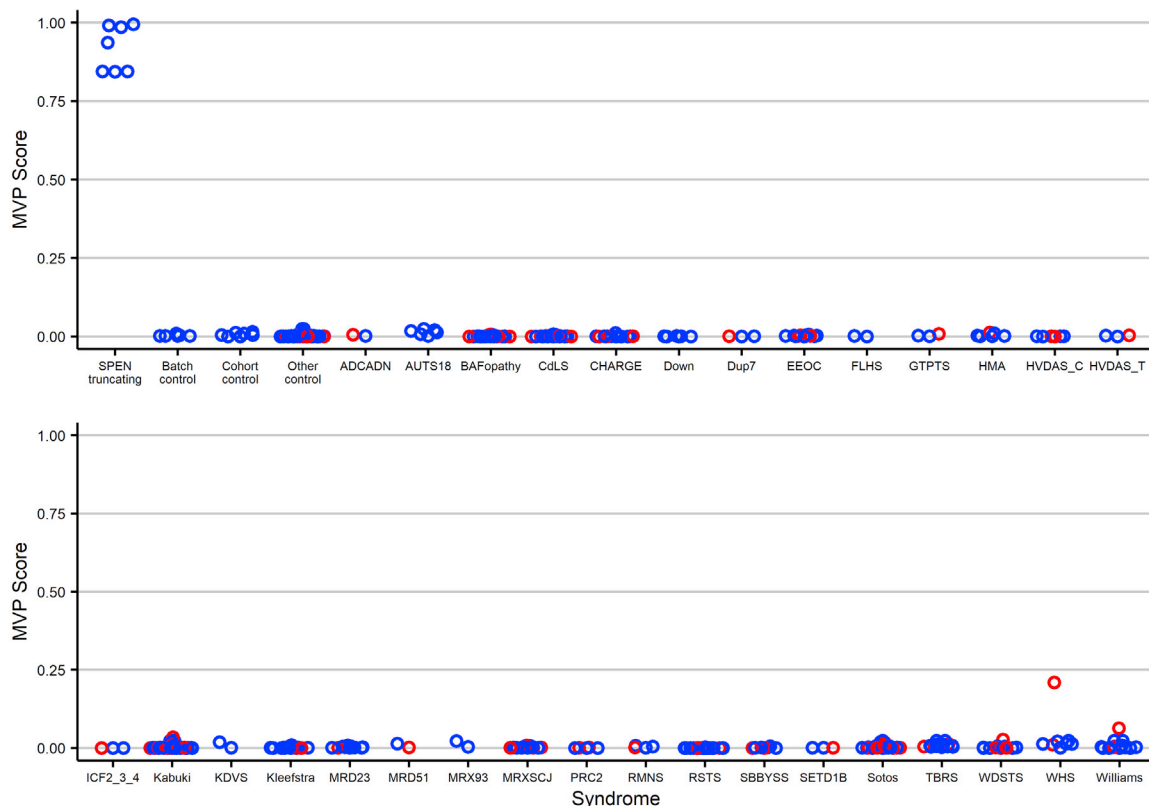


**Figure 4. The X chromosome episcapature in females with *SPEN*-truncating mutations differs from subjects with other neurodevelopmental disorders**

Blue samples (75%), including the *SPEN*-mutated samples and batch controls, were used for training and red samples (25%) were used for testing. Classification of female samples showed that the identified episcapature has high specificity, and no *SPEN* non-mutated samples have high scores.

preponderance in females. Obesity seems to worsen with age and was more common in adult females. Although additional independent studies are required to confirm this observation, it should be noted that obesity has also been described in individuals with distal 1p36 deletions, and a major locus contributes to this feature at 1p36.33.<sup>21</sup> Our finding suggests that at least two distinct loci for obesity, including one represented by *SPEN*, map to 1p36. Recently, a central and autonomous role of *SPEN* in the control of metabolism and energy balance was reported.<sup>72</sup> In *Spn*-deficient fruit fly larvae, lipid catabolism is impaired in fat storage cells because of impaired fatty acid catabolism and  $\beta$ -oxidation and is associated with increased adiposity, decreased lipase expression, and depletion of L-carnitine.<sup>73</sup> These findings suggest a model in which the increased food intake is an attempt to compensate for a condition of “perceived starvation” resulting from an inability to access to energy stores.<sup>72</sup> The possibility that a similar energetic metabolism dysregulation may underlie the increased age-related BMI and obesity in subjects with truncating *SPEN* mutations requires further investigation. The sex-biased distribution of obese subjects in the studied cohort may ultimately be tied to *SPEN*’s role as an estrogen-inducible cofactor in nuclear hormone receptor

activation/repression. Specifically, *SPEN* functions as a tumor-suppressor protein in ER-positive breast cancer cells, physically interacts with the estrogen receptor- $\alpha$  (ER $\alpha$ ), and is a potent sensitizer to tamoxifen in ER $\alpha$ -positive breast cancer cells.<sup>74,75</sup> It is well known that ERs (and in particular ER $\alpha$ ) are important regulators of energy intake and expenditure.<sup>76</sup> On the basis of these findings, a defective *SPEN*-mediated ER $\alpha$  function could explain female predisposition to obesity because estrogen sensitization could be a trigger to metabolic dysregulation and a consequential increase in BMI.

It has recently been demonstrated that *SPEN* is essential for initiating gene silencing on the X chromosome in preimplantation mouse embryos and in embryonic stem cells.<sup>68</sup> Specifically, *SPEN* acts as a molecular integrator, bridging Xist RNA with the transcription machinery, nucleosome remodelers, and histone deacetylases at active enhancers and promoters.<sup>68</sup> Consistent with this role, our methylome analyses documented that *SPEN* haploinsufficiency does not considerably affect the overall methylation status of the genome but is associated with a distinctive X chromosome episcapature in affected females. This finding is a paradigm of an X chromosome-specific episcapature that could be used to classify individuals with NDD. This suggests that searching for a sex-specific

DNA-methylation effect in previously unresolved cases may increase diagnostic yields.

1p36 deletions are highly variable in presentation and severity, mainly depending on size and position of the involved genomic region.<sup>14</sup> Deletions encompassing the distal critical region represent the far most common form of 1p36 deletions, and their relatively homogeneous phenotype has been well delineated. The phenotype of subjects with deletions involving the proximal region is more difficult to define given the small number of reported individuals, the variable size of the genomic regions involved, and the frequent inclusion of all or part of the distal critical region. We conclude that *SPEN* haploinsufficiency causes a recognizable syndromic NDD and represents a major contributor to the conditions associated with 1p36 deletions encompassing 1p36.21p36.13.

### Data and code availability

WES datasets have not been deposited in a public repository because of privacy and ethical restrictions but will be made available on request. All variants have been submitted to ClinVar (ClinVar: SCV001468518–SCV001468547) or DECIPHER (DECIPHER: 280862 and 286415).

### Acknowledgments

The authors thank the participating families and Claudia Nardini (Ospedale Pediatrico Bambino Gesù, Rome) and Serenella Venanzi (Istituto Superiore di Sanità, Rome) for technical assistance. This work was supported, in part, by Fondazione Bambino Gesù (*Vite Coraggiose* to M.T.), Italian Ministry of Health (CCR-2017-23669081 and RCR-2020-23670068\_001 to M.T.; RF-2018-12366931 to F.C.R. and B.D.; RC 11/16-Institute for Maternal and Child Health IRCCS Burlo Garofolo and RCR-2019-23669117\_001 to F.F., L.M., and P.G.), Netherlands Organisation for Scientific Research (ZonMW Veni) (grant 91617021 to T.S.B.), Brain & Behavior Research Foundation (NARSAD Young Investigator Grant to T.S.B.), NIH (R01HD098458 to D.A.S.), and Genome Canada (Genomic Applications Partnership Program grant to B.S.). Sequencing and data analysis of subject 14 were provided by the Broad Institute of MIT and Harvard Center for Mendelian Genomics and was funded by the National Human Genome Research Institute, National Eye Institute, and National Heart, Lung, and Blood Institute (UM1 HG008900) and by the National Human Genome Research Institute (R01 HG009141). Sequencing and data analyses of subjects 33 and 34 were supported by the NIH (R01MH101221 to E.E.E.) and Simons Foundation (SFARI #608045 to E.E.E.). The Deciphering Developmental Disorders (DDD) study presents independent research commissioned by the Health Innovation Challenge Fund (grant HICF-1009-003). This study makes use of DECIPHER, which is funded by the Wellcome. This work has been carried out in the frame of the ERN-ITHACA research activities.

### Declaration of interests

M.D., K.Mc., K.G.M., and A.T. are employees of GeneDx. All the other authors declare no competing interests.

Received: December 7, 2020

Accepted: January 26, 2021

Published: February 16, 2021

### Supplemental information

Supplemental information can be found online at <https://doi.org/10.1016/j.ajhg.2021.01.015>.

### Web resources

Annovar, <http://www.openbioinformatics.org/annovar/>

BrainSpan database, <http://www.brainspan.org>

ClinVar, <https://www.ncbi.nlm.nih.gov/clinvar/>

dbNSFP, <https://sites.google.com/site/jpopen/dbNSFP>

DECIPHER, <https://decipher.sanger.ac.uk/>

Denovo-db, <https://denovo-db.gs.washington.edu>

gnomAD, <https://gnomad.broadinstitute.org/>

InterVar, <http://wintervar.wglab.org>

Online Mendelian Inheritance in Man (OMIM), <https://omim.org/>

### References

1. Vissers, L.E., de Ligt, J., Gilissen, C., Janssen, I., Stehouwer, M., de Vries, P., van Lier, B., Arts, P., Wieskamp, N., del Rosario, M., et al. (2010). A de novo paradigm for mental retardation. *Nat. Genet.* *42*, 1109–1112.
2. Maulik, P.K., Mascarenhas, M.N., Mathers, C.D., Dua, T., and Saxena, S. (2011). Prevalence of intellectual disability: a meta-analysis of population-based studies. *Res. Dev. Disabil.* *32*, 419–436.
3. Van Naarden Braun, K., Christensen, D., Doernberg, N., Schieve, L., Rice, C., Wiggins, L., Schendel, D., and Yeargin-Allsopp, M. (2015). Trends in the prevalence of autism spectrum disorder, cerebral palsy, hearing loss, intellectual disability, and vision impairment, metropolitan atlanta, 1991-2010. *PLoS ONE* *10*, e0124120.
4. Vissers, L.E., Gilissen, C., and Veltman, J.A. (2016). Genetic studies in intellectual disability and related disorders. *Nat. Rev. Genet.* *17*, 9–18.
5. Shapira, S.K., McCaskill, C., Northrup, H., Spikes, A.S., Elder, F.F., Sutton, V.R., Korenberg, J.R., Greenberg, F., and Shaffer, L.G. (1997). Chromosome 1p36 deletions: the clinical phenotype and molecular characterization of a common newly delineated syndrome. *Am. J. Hum. Genet.* *61*, 642–650.
6. Shaffer, L.G., and Lupski, J.R. (2000). Molecular mechanisms for constitutional chromosomal rearrangements in humans. *Annu. Rev. Genet.* *34*, 297–329.
7. Heilstedt, H.A., Ballif, B.C., Howard, L.A., Kashork, C.D., and Shaffer, L.G. (2003a). Population data suggest that deletions of 1p36 are a relatively common chromosome abnormality. *Clin. Genet.* *64*, 310–316.
8. Shimada, S., Shimojima, K., Okamoto, N., Sangu, N., Hirasawa, K., Matsuo, M., Ikeuchi, M., Shimakawa, S., Shimizu, K., Mizuno, S., et al. (2015). Microarray analysis of 50 patients reveals the critical chromosomal regions responsible for 1p36 deletion syndrome-related complications. *Brain Dev.* *37*, 515–526.
9. Battaglia, A., Hoyme, H.E., Dallapiccola, B., Zackai, E., Hudgins, L., McDonald-McGinn, D., Bahi-Buisson, N., Romano,

- C., Williams, C.A., Brailey, L.L., et al. (2008). Further delineation of deletion 1p36 syndrome in 60 patients: a recognizable phenotype and common cause of developmental delay and mental retardation. *Pediatrics* *121*, 404–410.
10. Heilstedt, H.A., Ballif, B.C., Howard, L.A., Lewis, R.A., Stal, S., Kashork, C.D., Bacino, C.A., Shapira, S.K., and Shaffer, L.G. (2003b). Physical map of 1p36, placement of breakpoints in monosomy 1p36, and clinical characterization of the syndrome. *Am. J. Hum. Genet.* *72*, 1200–1212.
  11. Kang, S.H., Scheffer, A., Ou, Z., Li, J., Scaglia, F., Belmont, J., Lalani, S.R., Roeder, E., Enciso, V., Braddock, S., et al. (2007). Identification of proximal 1p36 deletions using array-CGH: a possible new syndrome. *Clin. Genet.* *72*, 329–338.
  12. Wu, Y.Q., Heilstedt, H.A., Bedell, J.A., May, K.M., Starkey, D.E., McPherson, J.D., Shapira, S.K., and Shaffer, L.G. (1999). Molecular refinement of the 1p36 deletion syndrome reveals size diversity and a preponderance of maternally derived deletions. *Hum. Mol. Genet.* *8*, 313–321.
  13. Gajecka, M., Mackay, K.L., and Shaffer, L.G. (2007). Monosomy 1p36 deletion syndrome. *Am. J. Med. Genet. C. Semin. Med. Genet.* *145C*, 346–356.
  14. Jordan, V.K., Zaveri, H.P., and Scott, D.A. (2015). 1p36 deletion syndrome: an update. *Appl. Clin. Genet.* *8*, 189–200.
  15. Rosenfeld, J.A., Crolla, J.A., Tomkins, S., Bader, P., Morrow, B., Gorski, J., Troxell, R., Forster-Gibson, C., Cilliers, D., Hislop, R.G., et al. (2010). Refinement of causative genes in monosomy 1p36 through clinical and molecular cytogenetic characterization of small interstitial deletions. *Am. J. Med. Genet. A* *152A*, 1951–1959.
  16. Windpassinger, C., Kroisel, P.M., Wagner, K., and Petek, E. (2002). The human gamma-aminobutyric acid A receptor delta (GABRD) gene: molecular characterisation and tissue-specific expression. *Gene* *292*, 25–31.
  17. Dibbens, L.M., Feng, H.J., Richards, M.C., Harkin, L.A., Hodgson, B.L., Scott, D., Jenkins, M., Petrou, S., Sutherland, G.R., Scheffer, I.E., et al. (2004). GABRD encoding a protein for extra- or peri-synaptic GABAA receptors is a susceptibility locus for generalized epilepsies. *Hum. Mol. Genet.* *13*, 1315–1319.
  18. Arndt, A.K., Schafer, S., Drenckhahn, J.D., Sabeh, M.K., Plovie, E.R., Caliebe, A., Klopocki, E., Musso, G., Werdich, A.A., Kalwa, H., et al. (2013). Fine mapping of the 1p36 deletion syndrome identifies mutation of PRDM16 as a cause of cardiomyopathy. *Am. J. Hum. Genet.* *93*, 67–77.
  19. McCormack, K., Connor, J.X., Zhou, L., Ho, L.L., Ganetzky, B., Chiu, S.-Y., and Messing, A. (2002). Genetic analysis of the mammalian K<sup>+</sup> channel beta subunit Kvbeta 2 (Kcnab2). *J. Biol. Chem.* *277*, 13219–13228.
  20. Zaveri, H.P., Beck, T.F., Hernández-García, A., Shelly, K.E., Montgomery, T., van Haeringen, A., Anderlid, B.M., Patel, C., Goel, H., Houge, G., et al. (2014). Identification of critical regions and candidate genes for cardiovascular malformations and cardiomyopathy associated with deletions of chromosome 1p36. *PLoS ONE* *9*, e85600.
  21. D'Angelo, C.S., Kohl, I., Varela, M.C., de Castro, C.I.E., Kim, C.A., Bertola, D.R., Lourenço, C.M., and Koiffmann, C.P. (2010). Extending the phenotype of monosomy 1p36 syndrome and mapping of a critical region for obesity and hyperphagia. *Am. J. Med. Genet. A* *152A*, 102–110.
  22. Rudnik-Schöneborn, S., Zerres, K., Häusler, M., Lott, A., Krings, T., and Schüle, H.M. (2008). A new case of proximal monosomy 1p36, extending the phenotype. *Am. J. Med. Genet. A* *146A*, 2018–2022.
  23. Zoltewicz, J.S., Stewart, N.J., Leung, R., and Peterson, A.S. (2004). Atrophin 2 recruits histone deacetylase and is required for the function of multiple signaling centers during mouse embryogenesis. *Development* *131*, 3–14.
  24. Fregeau, B., Kim, B.J., Hernández-García, A., Jordan, V.K., Cho, M.T., Schnur, R.E., Monaghan, K.G., Juusola, J., Rosenfeld, J.A., Bhoj, E., et al. (2016). De Novo Mutations of RERE Cause a Genetic Syndrome with Features that Overlap Those Associated with Proximal 1p36 Deletions. *Am. J. Hum. Genet.* *98*, 963–970.
  25. Jordan, V.K., Fregeau, B., Ge, X., Giordano, J., Wapner, R.J., Balci, T.B., Carter, M.T., Bernat, J.A., Moccia, A.N., Srivastava, A., et al.; Undiagnosed Diseases Network (2018). Genotype-phenotype correlations in individuals with pathogenic RERE variants. *Hum. Mutat.* *39*, 666–675.
  26. Sierra, O.L., Cheng, S.L., Loewy, A.P., Charlton-Kachigian, N., and Towler, D.A. (2004). MINT, the Msx2 interacting nuclear matrix target, enhances Runx2-dependent activation of the osteocalcin fibroblast growth factor response element. *J. Biol. Chem.* *279*, 32913–32923.
  27. Carter, A.C., Xu, J., Nakamoto, M.Y., Wei, Y., Zarnegar, B.J., Shi, Q., Broughton, J.P., Ransom, R.C., Salhotra, A., Nagaraja, S.D., et al. (2020). Spen links RNA-mediated endogenous retrovirus silencing and X chromosome inactivation. *eLife* *9*, e54508.
  28. McHugh, C.A., Chen, C.K., Chow, A., Surka, C.F., Tran, C., McDonel, P., Pandya-Jones, A., Blanco, M., Burghard, C., Moradian, A., et al. (2015). The Xist lncRNA interacts directly with SHARP to silence transcription through HDAC3. *Nature* *521*, 232–236.
  29. Shi, Y., Downes, M., Xie, W., Kao, H.Y., Ordentlich, P., Tsai, C.C., Hon, M., and Evans, R.M. (2001). Sharp, an inducible cofactor that integrates nuclear receptor repression and activation. *Genes Dev.* *15*, 1140–1151.
  30. Lane, M.E., Elend, M., Heidmann, D., Herr, A., Marzodko, S., Herzig, A., and Lehner, C.F. (2000). A screen for modifiers of cyclin E function in *Drosophila melanogaster* identifies Cdk2 mutations, revealing the insignificance of putative phosphorylation sites in Cdk2. *Genetics* *155*, 233–244.
  31. Jain, P., Zhang, S., Kanagal-Shamanna, R., Ok, C.Y., Nomie, K., Gonzalez, G.N., Gonzalez-Pagan, O., Hill, H.A., Lee, H.J., Fayad, L., et al. (2020). Genomic profiles and clinical outcomes of de novo blastoid/pleomorphic MCL are distinct from those of transformed MCL. *Blood Adv.* *4*, 1038–1050.
  32. Liu, D., Yang, Y., Yan, A., and Yang, Y. (2020). SPOCD1 accelerates ovarian cancer progression and inhibits cell apoptosis via the PI3K/AKT pathway. *OncoTargets Ther.* *13*, 351–359.
  33. Kuang, B., Wu, S.C., Shin, Y., Luo, L., and Kolodziej, P. (2000). split ends encodes large nuclear proteins that regulate neuronal cell fate and axon extension in the *Drosophila* embryo. *Development* *127*, 1517–1529.
  34. Rebay, I., Chen, F., Hsiao, F., Kolodziej, P.A., Kuang, B.H., Laverty, T., Suh, C., Voas, M., Williams, A., and Rubin, G.M. (2000). A genetic screen for novel components of the Ras/Mitogen-activated protein kinase signaling pathway that interact with the yan gene of *Drosophila* identifies split ends, a new RNA recognition motif-containing protein. *Genetics* *154*, 695–712.
  35. Doroquez, D.B., Orr-Weaver, T.L., and Rebay, I. (2007). Split ends antagonizes the Notch and potentiates the EGFR signaling pathways during *Drosophila* eye development. *Mech. Dev.* *124*, 792–806.

36. Oswald, F., Winkler, M., Cao, Y., Astrahantseff, K., Bourteele, S., Knöchel, W., and Borggrefe, T. (2005). RBP-Jkappa/SHARP recruits CtBP/CtBP corepressors to silence Notch target genes. *Mol. Cell. Biol.* *25*, 10379–10390.
37. Feng, Y., Bommer, G.T., Zhai, Y., Akyol, A., Hinoi, T., Winer, I., Lin, H.V., Cadigan, K.M., Cho, K.R., and Fearon, E.R. (2007). *Drosophila* split ends homologue SHARP functions as a positive regulator of Wnt/beta-catenin/T-cell factor signaling in neoplastic transformation. *Cancer Res.* *67*, 482–491.
38. Chen, F., and Rebay, I. (2000). split ends, a new component of the *Drosophila* EGF receptor pathway, regulates development of midline glial cells. *Curr. Biol.* *10*, 943–946.
39. Ariyoshi, M., and Schwabe, J.W. (2003). A conserved structural motif reveals the essential transcriptional repression function of Spen proteins and their role in developmental signaling. *Genes Dev.* *17*, 1909–1920.
40. Kuroda, K., Han, H., Tani, S., Tanigaki, K., Tun, T., Furukawa, T., Taniguchi, Y., Kurooka, H., Hamada, Y., Toyokuni, S., and Honjo, T. (2003). Regulation of marginal zone B cell development by MINT, a suppressor of Notch/RBP-J signaling pathway. *Immunity* *18*, 301–312.
41. Yabe, D., Fukuda, H., Aoki, M., Yamada, S., Takebayashi, S., Shinkura, R., Yamamoto, N., and Honjo, T. (2007). Generation of a conditional knockout allele for mammalian Spen protein Mint/SHARP. *Genesis* *45*, 300–306.
42. Iossifov, I., O’Roak, B.J., Sanders, S.J., Ronemus, M., Krumm, N., Levy, D., Stessman, H.A., Witherspoon, K.T., Vives, L., Patterson, K.E., et al. (2014). The contribution of de novo coding mutations to autism spectrum disorder. *Nature* *515*, 216–221.
43. Krumm, N., Turner, T.N., Baker, C., Vives, L., Mohajeri, K., Witherspoon, K., Raja, A., Coe, B.P., Stessman, H.A., He, Z.X., et al. (2015). Excess of rare, inherited truncating mutations in autism. *Nat. Genet.* *47*, 582–588.
44. Yuen, R.K., Merico, D., Cao, H., Pellecchia, G., Alipanahi, B., Thiruvahindrapuram, B., Tong, X., Sun, Y., Cao, D., Zhang, T., et al. (2016). Genome-wide characteristics of *de novo* mutations in autism. *NPJ Genom. Med.* *1*, 160271–1602710.
45. Deciphering Developmental Disorders Study (2017). Prevalence and architecture of de novo mutations in developmental disorders. *Nature* *542*, 433–438.
46. Kaplanis, J., Samocha, K.E., Wiel, L., Zhang, Z., Arvai, K.J., Eberhardt, R.Y., Gallone, G., Lelieveld, S.H., Martin, H.C., McRae, J.F., et al.; Deciphering Developmental Disorders Study (2020). Evidence for 28 genetic disorders discovered by combining healthcare and research data. *Nature* *586*, 757–762.
47. Wang, T., Hoekzema, K., Vecchio, D., Wu, H., Sulovari, A., Coe, B.P., Gillentine, M.A., Wilfert, A.B., Perez-Jurado, L.A., Kvarnung, M., et al.; SPARK Consortium (2020). Large-scale targeted sequencing identifies risk genes for neurodevelopmental disorders. *Nat. Commun.* *11*, 4932.
48. de Ligt, J., Willemsen, M.H., van Bon, B.W., Kleefstra, T., Yntema, H.G., Kroes, T., Vulto-van Silfhout, A.T., Koolen, D.A., de Vries, P., Gilissen, C., et al. (2012). Diagnostic exome sequencing in persons with severe intellectual disability. *N. Engl. J. Med.* *367*, 1921–1929.
49. Farwell, K.D., Shahmirzadi, L., El-Khechen, D., Powis, Z., Chao, E.C., Tippin Davis, B., Baxter, R.M., Zeng, W., Mroske, C., Parra, M.C., et al. (2015). Enhanced utility of family-centered diagnostic exome sequencing with inheritance model-based analysis: results from 500 unselected families with undiagnosed genetic conditions. *Genet. Med.* *17*, 578–586.
50. Wright, C.F., Fitzgerald, T.W., Jones, W.D., Clayton, S., McRae, J.F., van Kogelenberg, M., King, D.A., Ambridge, K., Barrett, D.M., Bayzatinova, T., et al.; DDD study (2015). Genetic diagnosis of developmental disorders in the DDD study: a scalable analysis of genome-wide research data. *Lancet* *385*, 1305–1314.
51. Retterer, K., Juusola, J., Cho, M.T., Vitazka, P., Millan, F., Gibellini, F., Vertino-Bell, A., Smaoui, N., Neidich, J., Monaghan, K.G., et al. (2016). Clinical application of whole-exome sequencing across clinical indications. *Genet. Med.* *18*, 696–704.
52. Thevenon, J., Duffourd, Y., Masurel-Paulet, A., Lefebvre, M., Feillet, F., El Chehadah-Djebbar, S., St-Onge, J., Steinmetz, A., Huet, F., Chouchane, M., et al. (2016). Diagnostic odyssey in severe neurodevelopmental disorders: toward clinical whole-exome sequencing as a first-line diagnostic test. *Clin. Genet.* *89*, 700–707.
53. Thiffault, I., Cadieux-Dion, M., Farrow, E., Caylor, R., Miller, N., Soden, S., and Saunders, C. (2018). On the verge of diagnosis: Detection, reporting, and investigation of de novo variants in novel genes identified by clinical sequencing. *Hum. Mutat.* *39*, 1505–1516.
54. Boonsawat, P., Joset, P., Steindl, K., Oneda, B., Gogoll, L., Azzarello-Burri, S., Sheth, F., Datar, C., Verma, I.C., Puri, R.D., et al.; Undiagnosed Diseases Network (UDN) (2019). Elucidation of the phenotypic spectrum and genetic landscape in primary and secondary microcephaly. *Genet. Med.* *21*, 2043–2058.
55. Chatron, N., Cabet, S., Alix, E., Buenerd, A., Cox, P., Guibaud, L., Labalme, A., Marks, P., Osio, D., Putoux, A., et al. (2019). A novel lethal recognizable polymicrogyric syndrome caused by ATP1A2 homozygous truncating variants. *Brain* *142*, 3367–3374.
56. Motta, M., Pannone, L., Pantaleoni, F., Bocchinfuso, G., Radio, F.C., Cecchetti, S., Ciolfi, A., Di Rocco, M., Elting, M.W., Brilstra, E.H., et al. (2020). Enhanced MAPK1 Function Causes a Neurodevelopmental Disorder within the RASopathy Clinical Spectrum. *Am. J. Hum. Genet.* *107*, 499–513.
57. Wagner, M., Lévy, J., Jung-Klawitter, S., Bakhtiari, S., Monteiro, F., Maroofian, R., Bierhals, T., Hempel, M., Elmaleh-Bergès, M., Kitajima, J.P., et al. (2020). Loss of TNR causes a nonprogressive neurodevelopmental disorder with spasticity and transient opisthotonus. *Genet. Med.* *22*, 1061–1068.
58. Zanus, C., Costa, P., Faletta, F., Musante, L., Russo, A., Grazian, L., and Carrozzi, M. (2020). Description of a peculiar alternating ictal electroclinical pattern in a young boy with a novel SPATA5 mutation. *Epileptic Disord.* *22*, 659–663.
59. Sobreira, N., Schiettecatte, F., Valle, D., and Hamosh, A. (2015). GeneMatcher: a matching tool for connecting investigators with an interest in the same gene. *Hum. Mutat.* *36*, 928–930.
60. Firth, H.V., Richards, S.M., Bevan, A.P., Clayton, S., Corpas, M., Rajan, D., Van Vooren, S., Moreau, Y., Pettett, R.M., and Carter, N.P. (2009). DECIPHER: Database of Chromosomal Imbalance and Phenotype in Humans Using Ensembl Resources. *Am. J. Hum. Genet.* *84*, 524–533.
61. Kang, H.J., Kawasaki, Y.I., Cheng, F., Zhu, Y., Xu, X., Li, M., Sousa, A.M., Pletikos, M., Meyer, K.A., Sedmak, G., et al. (2011). Spatio-temporal transcriptome of the human brain. *Nature* *478*, 483–489.

62. Zhong, S., Zhang, S., Fan, X., Wu, Q., Yan, L., Dong, J., Zhang, H., Li, L., Sun, L., Pan, N., et al. (2018). A single-cell RNA-seq survey of the developmental landscape of the human prefrontal cortex. *Nature* 555, 524–528.
63. Pang, K., Wang, L., Wang, W., Zhou, J., Cheng, C., Han, K., Zoghbi, H.Y., and Liu, Z. (2020). Coexpression enrichment analysis at the single-cell level reveals convergent defects in neural progenitor cells and their cell-type transitions in neurodevelopmental disorders. *Genome Res.* 30, 835–848.
64. Parikshak, N.N., Luo, R., Zhang, A., Won, H., Lowe, J.K., Chandran, V., Horvath, S., and Geschwind, D.H. (2013). Integrative functional genomic analyses implicate specific molecular pathways and circuits in autism. *Cell* 155, 1008–1021.
65. Willsey, A.J., Sanders, S.J., Li, M., Dong, S., Tebbenkamp, A.T., Muhle, R.A., Reilly, S.K., Lin, L., Fertuzinhos, S., Miller, J.A., et al. (2013). Coexpression networks implicate human midfetal deep cortical projection neurons in the pathogenesis of autism. *Cell* 155, 997–1007.
66. Hormozdiari, F., Penn, O., Borenstein, E., and Eichler, E.E. (2015). The discovery of integrated gene networks for autism and related disorders. *Genome Res.* 25, 142–154.
67. Oswald, F., Kostezka, U., Astrahantseff, K., Bourteele, S., Dillinger, K., Zechner, U., Ludwig, L., Wilda, M., Hameister, H., Knöchel, W., et al. (2002). SHARP is a novel component of the Notch/RBP-Jkappa signalling pathway. *EMBO J.* 21, 5417–5426.
68. Dossin, F., Pinheiro, I., Żylicz, J.J., Roensch, J., Collombet, S., Le Saux, A., Chelmicki, T., Attia, M., Kapoor, V., Zhan, Y., et al. (2020). SPEN integrates transcriptional and epigenetic control of X-inactivation. *Nature* 578, 455–460.
69. Aref-Eshghi, E., Bend, E.G., Colaiacovo, S., Caudle, M., Chakrabarti, R., Napier, M., Brick, L., Brady, L., Carere, D.A., Levy, M.A., et al. (2019). Diagnostic Utility of Genome-wide DNA Methylation Testing in Genetically Unsolved Individuals with Suspected Hereditary Conditions. *Am. J. Hum. Genet.* 104, 685–700.
70. Aref-Eshghi, E., Kerkhof, J., Pedro, V.P., Barat-Houari, M., Ruiz-Pallares, N., Andrau, J.C., Lacombe, D., Van-Gils, J., Fergelot, P., Dubourg, C., et al.; Groupe DI France (2020). Evaluation of DNA Methylation Episignatures for Diagnosis and Phenotype Correlations in 42 Mendelian Neurodevelopmental Disorders. *Am. J. Hum. Genet.* 106, 356–370.
71. Monfort, A., Di Minin, G., Postlmayr, A., Freimann, R., Arieti, F., Thore, S., and Wutz, A. (2015). Identification of Spen as a Crucial Factor for Xist Function through Forward Genetic Screening in Haploid Embryonic Stem Cells. *Cell Rep.* 12, 554–561.
72. Hazegh, K.E., Nemkov, T., D'Alessandro, A., Diller, J.D., Monks, J., McManaman, J.L., Jones, K.L., Hansen, K.C., and Reis, T. (2017). An autonomous metabolic role for Spen. *PLoS Genet.* 13, e1006859.
73. Gillette, C.M., Hazegh, K.E., Nemkov, T., Stefanoni, D., D'Alessandro, A., Taliaferro, J.M., and Reis, T. (2020). Gene-Diet Interactions: Dietary Rescue of Metabolic Defects in *spen*-Depleted *Drosophila melanogaster*. *Genetics* 215, 887.
74. Légaré, S., Cavallone, L., Mamo, A., Chabot, C., Sirois, I., Magliocco, A., Klimowicz, A., Tonin, P.N., Buchanan, M., Keilty, D., et al. (2015). The Estrogen Receptor Cofactor SPEN Functions as a Tumor Suppressor and Candidate Biomarker of Drug Responsiveness in Hormone-Dependent Breast Cancers. *Cancer Res.* 75, 4351–4363.
75. Légaré, S., and Basik, M. (2016). Minireview: The Link Between ER $\alpha$  Corepressors and Histone Deacetylases in Tamoxifen Resistance in Breast Cancer. *Mol. Endocrinol.* 30, 965–976.
76. Heine, P.A., Taylor, J.A., Iwamoto, G.A., Lubahn, D.B., and Cooke, P.S. (2000). Increased adipose tissue in male and female estrogen receptor-alpha knockout mice. *Proc. Natl. Acad. Sci. USA* 97, 12729–12734.